

# Settling Time of Mesochronous Clock Retiming Circuits for Low Swing Interconnects

Naveen Kadavinti, Amitalok J. Budkuley, Dinesh K. Sharma

**Abstract**—Repeaterless low swing on-chip interconnects require clock synchronization circuits at the receiver to sample the incoming low swing data. While a clock of the correct frequency is generally available from the clock grid, the correct phase still needs to be recovered. Mesochronous retiming circuits are used to generate a sampling clock positioned at the center of the data eye. In this work, we discuss the settling behaviour of such mesochronous synchronizers. We first show that inter-symbol interference can cause an indefinite increase in the settling time of the synchronizer. This occurs when the initial phase of the clock is within the horizontally closed region of the data eye. Next, we model the synchronizer system as a Markov chain with absorbing states and determine the mean absorption time which is indicative of the mean settling time of the circuit. The model predictions match well with behavioural simulations of the synchronizer. Finally, we suggest ways to reduce the settling time.

**Index Terms**—Metastability, Mesochronous synchronizers, Inter-symbol interference, Low swing interconnect, Absorbing Markov chains.

## I. INTRODUCTION

Repeaterless interconnects with low swing on the line are required to continue the performance scaling of long interconnects while keeping the power consumption low [1]–[3]. Regenerative comparators are used at the receiver to convert the low swing input data to rail-rail levels. While these architectures outperform the repeater inserted links in speed, power as well as routing complexity, they have high latency which can be as high as multiple cycles. Hence, appropriate clock synchronization circuits are needed at the receiver to sample the data correctly [4], [5]. The front end of the synchronizer is a phase detector which senses the phase difference between the low swing input data and the sampling clock. The synchronizer can derive the sampling clock from the source clock (which is of the correct frequency) either by using a delay line [5] or by using phase interpolation [6]. This work discusses the settling time of these synchronizers in the presence of Inter-Symbol Interference (ISI).

Fig. 1 shows the block diagram of a repeaterless interconnect system. The delay of the interconnect is expressed as  $(n+\lambda)T$ , where  $n$  is a non negative integer,  $\lambda$  is a real number taking values in  $[0,1)$  and  $T$  is the system clock period. The initial phase error is a continuous variable taking values in  $[0, 2\pi)$ . When the initial phase error is less than  $\pi$  (more than  $\pi$ ), the circuit achieves lock by decreasing (increasing) the phase to  $0$  ( $2\pi$ ). The settling time of the synchronizer depends

The authors are with the Department of Electrical Engineering at the Indian Institute of Technology Bombay, Mumbai, India 400076. Emails: (naveen,amitalok,dinesh)@ee.iitb.ac.in

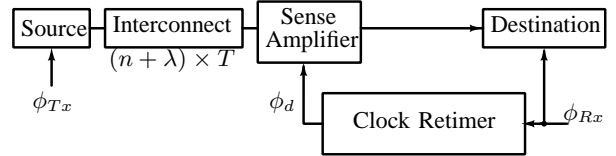


Fig. 1. Block diagram of a repeaterless low swing interconnect system.  $\phi_{Tx}$ : Transmitter clock,  $\phi_{Rx}$ : Receiver clock,  $\phi_d$ : retimed sampling clock,  $((n + \lambda) \times T)$ : Repeaterless interconnect delay, where  $n \in \mathbb{Z}^+$ ,  $\lambda \in \mathbb{R}$  &  $\lambda < 1$ ,  $T$ : system clock period.

on the gain of the system and the initial phase error. This settling time can be expressed as

$$t_s = T \frac{sC}{\alpha K_{PD} K_{VC} K_{CP}} \phi_{error} \quad (1)$$

where  $\alpha$  is the data activity factor,  $K_{PD}$ ,  $K_{VC}$  and  $K_{CP}$  are the gains of the phase detector, the phase modulator and the charge pump respectively, and  $\phi_{error}$  is the initial phase error. However, when the data is corrupt with inter-symbol interference (ISI), and when the initial phase error lies in a small window around  $\pi$ , this expression for the settling time is not valid. This is due to the fact that the output of the phase detector in these conditions is randomized by the jitter in the data and the phase error information is lost. This extends the settling time  $t_s$  indefinitely till the system escapes this *window of susceptibility*  $\mathcal{W}$ . The size of the window  $\mathcal{W}$  depends on the amount of ISI introduced by the interconnect.

Typical systems on chip can have hundreds of long interconnects [7], [8], and a horizontal eye opening of about 85% is not pessimistic [1], [3]. If the initial clock position is assumed to be uniformly distributed, then there is a 15% chance that the synchronizer wakes up with its initial phase in this window of uncertainty, making it important to study and understand this problem. Circuit level simulations show that the system can remain stuck in the window for thousands of cycles. Fig. 2 shows the eye diagram at the receiver input of a typical low swing interconnect. Here,  $T_w$  is the width of the window  $\mathcal{W}$ . Fig. 3 shows the control voltage of a coarse-fine type synchronizer [5] when the circuit is stuck with its clock in this window. The simulation was done in UMC 130 nm CMOS technology, with a 10 mm interconnect and a low swing current mode transmitter with capacitive pre-emphasis [1].

In this paper we study this phenomenon in detail and model the synchronizer system as a Markov chain with absorbing states. The transitions of the chain represent the phase corrections done by the synchronizer. The direction of phase update

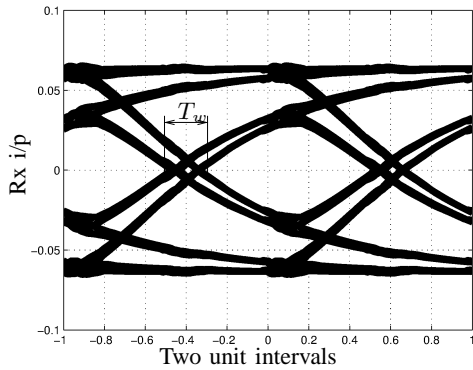


Fig. 2. Eye diagram at receiver input.

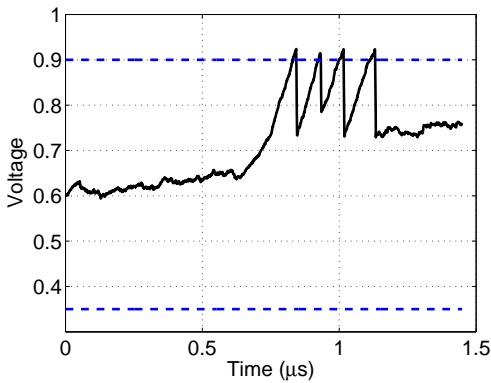


Fig. 3. Control voltage trajectory when initial sampling instant is within  $T_w$ .

in each cycle depends on the ISI, and hence, the input data. The model fits the data obtained from behavioural simulations and provides useful insights into the dynamics of the system. We show that by introducing a small mismatch in the relative strengths of the UP and DN updates the settling time can be reduced considerably. Alternately, an appropriately designed training sequence can bias the synchronizer at the receiver to one of the directions to reduce the settling time. These techniques are then confirmed with circuit level simulations.

The paper is organized as follows. Section II describes the working of phase detectors in the presence of inter-symbol interference and explains the increase in settling time. The modelling of the synchronizer as a Markov chain with absorbing states is described in Section III. Further, the effects of UP and DN mismatch on the settling time are also discussed. Simulation results and discussions are presented in Section IV. Section V then concludes the the paper.

## II. WORKING OF PHASE DETECTORS IN THE WINDOW OF SUSCEPTIBILITY

### A. The Alexander phase detector

The timing diagram of the Alexander phase detector is shown in Fig. 4 [9]. The phase detector takes 2 samples per bit period and takes a binary decision of shifting the clock to the right or left based on the last three samples. When there is no ISI, the phase detector consistently produces either UP or

DN pulses. Thus, for a given data activity factor the settling time can be calculated deterministically.

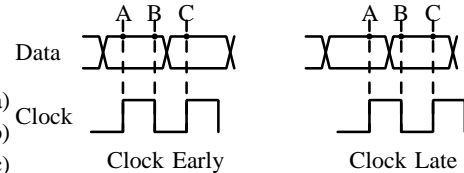


Fig. 4. The sampling instants of the Alexander phase detector.

Fig. 5 shows the timing diagram of the Alexander phase detector when the data is corrupt with ISI and the initial phase error is close to  $\pi$  radians. ISI in the interconnect causes jitter in the data. Hence, the sample of the data close to the data transition (which is the deciding sample) causes the phase detector to generate UP and DN signals depending solely on the data stream (ISI) and not on the average data arrival time. Thus, the phase detector loop can remain stuck in this region indefinitely.

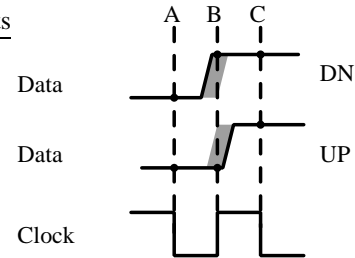


Fig. 5. The sampling instants of the Alexander phase detector.

### B. The Hogge phase detector

Linear phase detectors like the Hogge phase detector [10] will behave similar to binary phase detectors in the window of susceptibility. In Fig. 6 the characteristics of the Alexander and Hogge phase detector are depicted. The highlighted region shows the window of susceptibility, and within this window the variation of the gain of the phase detector is negligible. Hence, the analysis of the system behaviour in the window of susceptibility is applicable to both these types of phase detectors .

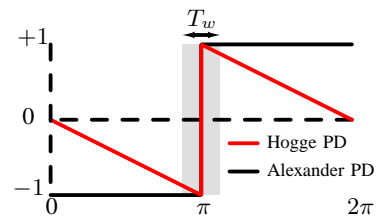


Fig. 6. The characteristic of linear and binary phase detectors. Highlighted region indicates the window of susceptibility. The phase detector gains are normalized.

### III. MARKOV MODEL OF THE SYNCHRONIZER

When the binary phase detector is used, the phase detector produces UP/DN pulses every data transition which are converted to an analog control voltage using a charge pump. The control voltage is used to delay the clock (either using a phase interpolator or a delay line). Since the input is binary, the output phase is quantized. Hence, we can discretize the clock position to the step size ( $\delta$ ) of the phase detector loop update. We are particularly interested in the region where the input data eye is closed.

We shall model the system assuming that the ISI is limited to a single previous bit. Fig. 7 illustrates a diagram with 1 bit ISI. In this case, the data signal follows one of two distinct traces. Here,  $t_i$  is the initial sampling instant of the clock,

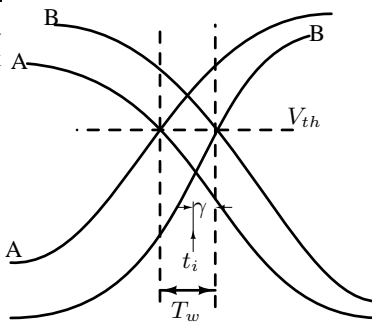


Fig. 7. Cartoon of an eye diagram with 1 bit ISI (Only horizontally closed region).

$T_w$  is the width of the window of susceptibility (which is the horizontally closed region of the data eye),  $\gamma$  is the distance to the right edge of the window and  $V_{th}$  is the threshold of the samplers in the phase detector.

Assuming that the source outputs 1 and 0 with equal probability, we list the bit combinations that will result in traces A and B respectively which are shown in Table III.

TABLE I  
POSSIBLE SEQUENCES AND DATA TRACES FOR 1 BIT ISI.

$b_{-2}$	$b_{-1}$	$b_0$	Trace	Action
0	0	0	-	NA
0	0	1	Trace B	LT
0	1	0	Trace A	RT
0	1	1	-	NA
1	0	0	-	NA
1	0	1	Trace A	RT
1	1	0	Trace B	LT
1	1	1	-	NA

Here *LT* and *RT* indicate that the clock is shifted to the left and to the right respectively by a step of size  $\delta$ . *NA* indicates no corrective action in that cycle. When all traces are equally likely,  $P(RT) = 0.25 = P(LT)$  and  $P(NA) = 0.5$ . Note that the system escapes the window of susceptibility when, for the first time, either  $(n_R - n_L)\delta \geq \gamma$  or  $(n_L - n_R)\delta \geq (T_w - \gamma)$ . Here,  $n_R$  and  $n_L$  are the total number of times the clock

position has been shifted to the right and to the left respectively from startup.

We model this system as a one dimensional Markov chain. The states of the Markov chain are the positions of the sampling clock in the window of susceptibility. Once the clock position escapes this window, time taken to lock to center of the eye can be calculated from Eq. 1. Thus, the edge positions of the window are modeled as absorbing states. This makes the model is a Markov chain with absorbing states. Fig. 8 shows the state diagram of the Markov chain for this system. By knowing the state space and transition probabilities of a Markov chain, one can calculate the mean time to absorption from any initial state [11]. We present the details of the calculations of the mean time to absorption (as well as its variance) in Appendix A.

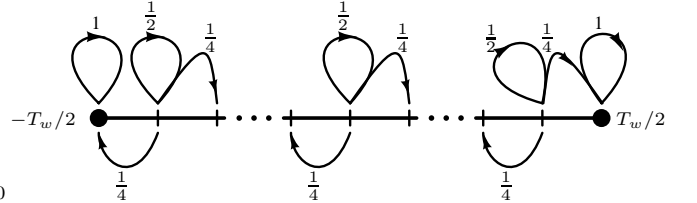


Fig. 8. Model of the synchronizer as a Markov chain with absorbing states.

The combined plots of the mean time to absorption for the 1 bit ISI example obtained from behavioural simulations and Markov model predictions are shown in Fig. 9. The model predictions were computed by solving for the mean absorption time of the Markov chain using a linear equation solver, while the behavioural simulations were done using VerilogA. As one would expect the settling time is maximum when the initial sampling phase is at the center of the window of susceptibility.

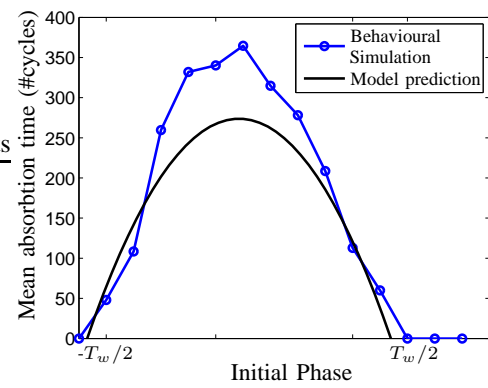


Fig. 9. Absorption time as predicted from the Markov model and from behavioural simulations. Each data point in the behavioural simulation is an average of 100 runs.

#### A. Effect of offsets in the sampler

Offsets in the sampling flip flops of the phase detector can increase the size of the window of susceptibility. An eye diagram illustrating the effect of offset in the sampler is depicted in Fig. 10. Note that the offsets directly increase the size of the window of susceptibility.

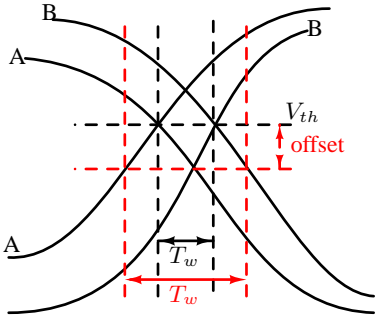


Fig. 10. Illustration of the effect of sampler offsets on the window of susceptibility.

#### B. Variance of the time to absorption and effect of UP and DN mismatch

Fig. 11 shows the mean time to absorption as a function of initial sampling phase, when the step sizes for the left and right shifts are (i) equal and (ii) mismatched by 10%.

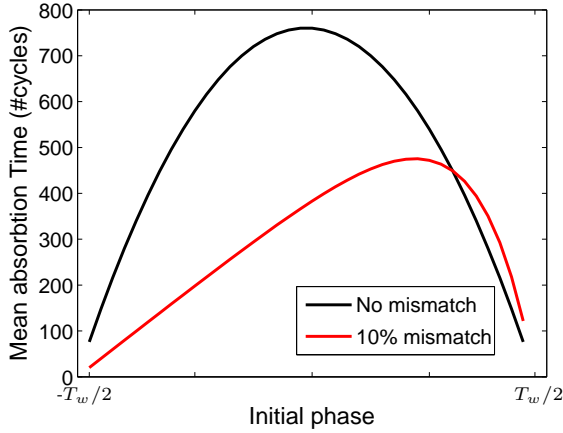


Fig. 11. Mean time to absorption with and without mismatch in the left and right shift weights.

Note that a 10% mismatch in the step size of the left/right shift reduces the mean absorption time by upto 40%. The variance of the time to absorption is of even higher significance as revealed in Fig. 12. Here we see that a small asymmetry in the left and right shift probabilities results in a significant reduction in the variance of the absorption time. To exploit this, we deliberately introduce a mismatch in the UP/DN strengths of the charge pump in the synchronizer to reduce the settling time. Alternately, if allowed by the system, a training sequence that introduces a similar mismatch can be used to reduce the convergence time.

#### IV. RESULTS AND DISCUSSIONS

As discussed before, typical systems on chip can have hundreds of long interconnects and a horizontal eye opening of about 85% results in a 15% chance that a synchronizer wakes up with its initial clock in the window of susceptibility. We use an implementation of a 10mm interconnect with a capacitively coupled transmitter in UMC 130 nm CMOS technology for the

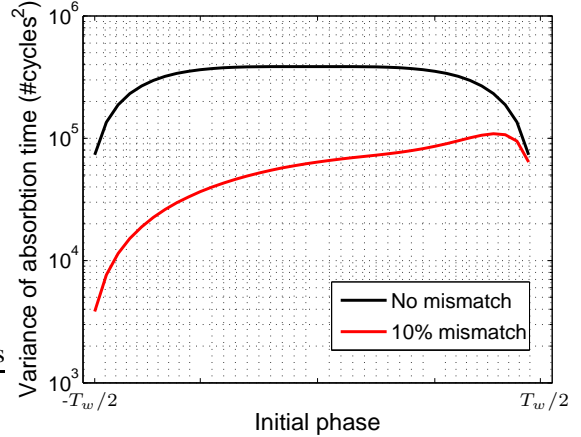


Fig. 12. Variance of the time to absorption for a symmetric Markov chain and for a chain with a 10% bias to left shift. Note that the y-axis is log scale.

simulation experiments. As was shown earlier in Fig. 3, the circuit can remain stuck in the window of susceptibility  $\mathcal{W}$  for thousands of cycles. Simulation results of the suggested techniques for reducing the settling time are discussed in this section.

#### A. Reduction in settling time with charge pump mismatch

Fig. 13 shows the reduction in the settling time of the synchronizer with the introduction of a 10% mismatch in the UP and DN currents of the charge pump. With identical initial conditions, a 10% mismatch results in >80% reduction in the time taken to exit the window of susceptibility.

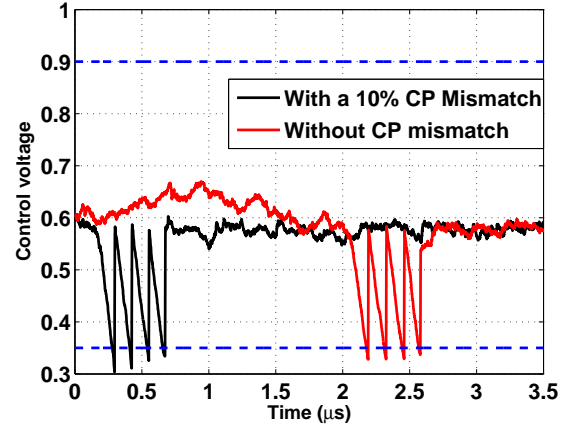


Fig. 13. Control voltage when initial phase error  $\sim \pi$  radians

Charge pump mismatch can result in increased jitter once the circuit has locked. Hence, if good jitter performance is desired, the introduced mismatch can be switched off after lock has been achieved.

#### B. Reduction in settling time with training sequence

A training sequence that biases the system to either one of the directions can be used to reduce the settling time. One such

training sequence is "...0010011100100111...". Note that since the sequence has a minimum run length of 1 bit for a logic '1' and 2 bits for logic '0', the ISI for logic '1' is always more than that for logic '0'. Hence, the phase detector's output in the window of susceptibility is biased towards the left. In Fig. 14, we plot the settling time when the above training sequence is used as well as with random equiprobable binary sequence. Notice the considerable reduction in the settling time when we use the deliberately biased training sequence. One could also use an alternating 1/0 training sequence which reduces the jitter due to ISI to zero. However, random uncorrelated jitter between the transmitter and receiver clocks will still result in a non-zero size of the window of susceptibility.

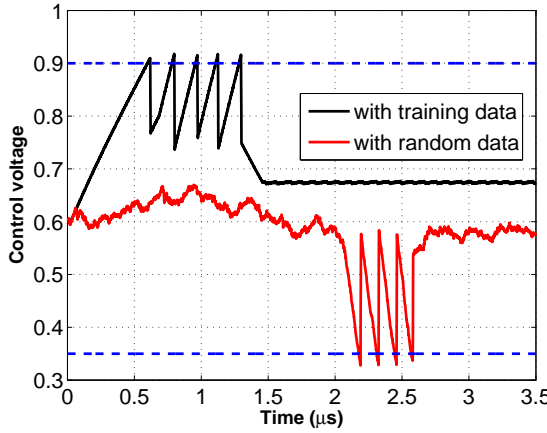


Fig. 14. Control voltage when initial phase error  $\sim \pi$  radians

## V. CONCLUSION

We have discussed how ISI can cause the settling time of mesochronous synchronizers to increase indefinitely. We model the system as a Markov chain with absorbing states. The model predictions of the settling time in terms of the mean absorption time of the Markov chain match well with behavioural simulations. We also suggest ways to considerably reduce the settling time by introducing a relative mismatch in the phase update steps in either direction. This can be achieved by introducing a mismatch in the charge pump or by using appropriately designed training data.

## APPENDIX A

### CALCULATION OF THE MEAN TIME TO ABSORPTION OF A MARKOV CHAIN

The state diagram of the Markov chain representation of the synchronizer system is shown in Fig. 8. The states corresponding to  $-T_w/2$  and  $T_w/2$ , which are at the edges of the window of susceptibility, are absorbing states. The probability

transition matrix  $P$  for this Markov chain can be written as

$$P = \begin{bmatrix} 1 & 0 & 0 & 0 & \cdots & 0 \\ \frac{1}{4} & \frac{1}{2} & \frac{1}{4} & 0 & \cdots & 0 \\ 0 & \frac{1}{4} & \frac{1}{2} & \frac{1}{4} & \cdots & 0 \\ \vdots & & & \ddots & & \vdots \\ 0 & \cdots & & 0 & \frac{1}{4} & \frac{1}{2} & \frac{1}{4} \\ 0 & \cdots & & 0 & 0 & 0 & 1 \end{bmatrix}.$$

To calculate the mean time to absorption (and the variance of the time to absorption), we first write the matrix in the canonical form [11]. This is obtained by reordering the matrix entries to separately aggregate all the transient states and all the absorbing states. This can be written as

$$P = \left[ \begin{array}{c|c} Q & R \\ \hline 0 & I \end{array} \right] = \left[ \begin{array}{ccccc|cc} \frac{1}{2} & \frac{1}{4} & 0 & 0 & \cdots & 0 & \frac{1}{4} & 0 \\ \frac{1}{4} & \frac{1}{2} & \frac{1}{4} & 0 & \cdots & 0 & 0 & 0 \\ \vdots & & & \ddots & & \vdots & \vdots & \vdots \\ 0 & \cdots & & & & \frac{1}{4} & \frac{1}{2} & 0 & \frac{1}{4} \\ \hline 0 & \cdots & & 0 & 0 & 1 & 0 \\ 0 & \cdots & & 0 & 0 & 0 & 1 \end{array} \right].$$

Here  $Q$  is square matrix which captures the transitions from one transient state to another transient state,  $R$  captures the transitions from transient states to absorbing states and  $I$  is an identity matrix. The fundamental matrix  $N$  can be computed using the equation

$$N = (I_t - Q)^{-1}.$$

Here,  $I_t$  is an identity matrix of same dimensions as  $Q$ . Conditioned on the starting position, the mean time to absorption (in terms of the number of steps) is calculated using the following equation.

$$T^{mean} = NC.$$

where,  $C$  is a column vector with number of columns equal to the number of transient states, and with all entries as 1.

The variance of the time to absorption (in terms of number of steps), conditioned on the starting position, is calculated as

$$T_{var} = (2N - I_t) \times T^{mean} - T_{sq}^{mean}.$$

Here,  $T_{sq}^{mean}$  is obtained by squaring all the elements of  $T^{mean}$ .

## REFERENCES

- [1] E. Mensink, D. Schinkel, E.A.M. Klumperink, E. van Tuijl, and B. Nauta, "Power efficient gigabit communication over capacitively driven rc-limited on-chip interconnects," *IEEE J. Solid-State Circuits*, vol. 45, no. 2, pp. 447–457, Feb. 2010.
- [2] R. Ho, T. Ono, F. Liu, R. Hopkins, A. Chow, J. Schauer, and R. Drost, "High-speed and low-energy capacitively-driven on-chip wires," in *IEEE Int. Solid State Circuits Conf. (ISSCC) Dig. of Tech. Papers*, 2007, pp. 412–414.

- [3] Byungsub Kim and V. Stojanovic and, "An energy-efficient equalized transceiver for RC-dominant channels," *IEEE J. Solid-State Circuits*, vol. 45, no. 6, pp. 1186–1197, June 2010.
- [4] S. H. Lee, S. K. Lee, B. Kim, H. J. Park, and J. Y. Sim, "Current-mode transceiver for silicon interposer channel," *IEEE J. Solid-State Circuits*, vol. 49, no. 9, pp. 2044–2053, Sept 2014.
- [5] N. Kadavinti, M. S. Baghini, and D. K. Sharma, "A clock Synchronizer for repeaterless low swing on-chip links," *ArXiv e-prints*, Oct. 2015, <http://arxiv.org/abs/1510.04241>.
- [6] R. Kreienkamp, Ulrich Langmann, C. Zimmermann, T. Aoyama, and H. Siedhoff, "A 10Gb/s CMOS clock and data recovery circuit with an analog phase interpolator," *IEEE J. Solid-State Circuits*, vol. 40, no. 3, pp. 736–743, March 2005.
- [7] J. W. Joyner, P. Zarkesh-Ha, and J. D. Meindl, "A stochastic global net-length distribution for a three-dimensional system-on-a-chip (3d-soc)," in *Proc. of the 14th Annual IEEE Int. ASIC/SOC Conf.*, 2001, pp. 147–151.
- [8] P. Zarkesh-Ha and J.D. Meindl, "Stochastic net length distributions for global interconnects in a heterogeneous system-on-a-chip," in *Symp. VLSI Technology, 1998. Digest of Technical Papers. 1998 Symposium on*, June 1998, pp. 44–45.
- [9] J.D.H. Alexander, "Clock recovery from random binary signals," *Electronics Letters*, vol. 11, no. 22, pp. 541–542, October 1975.
- [10] C. R. Hogge, "A self correcting clock recovery circuit," *IEEE Trans. Electron Devices*, vol. 32, no. 12, pp. 2704–2706, Dec 1985.
- [11] J.G. Kemeny and J.L. Snell, "Finite Markov Chains: With a New Appendix. Generalization of a Fundamental Matrix", Undergraduate Texts in Mathematics. Springer New York, 1983.